Bioorganic & Medicinal Chemistry Letters 21 (2011) 1871–1875

Contents lists available at ScienceDirect

Bioorganic & Medicinal Chemistry Letters

journal homepage: www.elsevier.com/locate/bmcl

Synthesis and SAR studies of novel 2-(4-oxo-2-aryl-quinazolin-3(4*H*)-yl) acetamide vasopressin V_{1b} receptor antagonists

Susan E. Napier [b,*], Jeffrey J. Letourneau [a,*], Nasrin Ansari [a], Douglas S. Auld [a], James Baker [c], Stuart Best [c], Leigh Campbell-Wan [c], Jui-Hsiang Chan [a], Mark Craighead [d], Hema Desai [a], Katharine A. Goan [d], Koc-Kan Ho [a], Ellen G. J. Hulskotte [e], Cliona P. MacSweeney [c], Rachel Milne [d], J. Richard Morphy [b], Irina Neagu [a], Michael H. J. Ohlmeyer [a], Ard W. M. M. Peeters [e], Jeremy Presland [d], Chris Riviello [a], Ge S. F. Ruigt [e], Fiona J. Thomson [d], Heather A. Zanetakos [a], Jiuqiao Zhao [a], Maria L. Webb [a]

[a] *Ligand Pharmaceuticals, Inc., 3000 Eastpark Boulevard, Cranbury, NJ 08512, USA*
[b] *Department of Chemistry, MSD, Newhouse, Lanarkshire ML1 5SH, UK*
[c] *Department of Pharmacology, MSD, Newhouse, Lanarkshire ML1 5SH, UK*
[d] *Department of Molecular Pharmacology, MSD, Newhouse, Lanarkshire ML1 5SH, UK*
[e] *Department of Clinical Research and Development, MSD, 5340BH Oss, The Netherlands*

ARTICLE INFO

Article history:
Received 19 October 2010
Revised 14 December 2010
Accepted 16 December 2010
Available online 21 December 2010

Keywords:
Vasopressin
HPA axis

ABSTRACT

Synthesis and structure–activity relationships (SAR) of a novel series of vasopressin V_{1b} (V_3) antagonists are described. 2-(4-Oxo-2-aryl-quinazolin-3(4*H*)-yl)acetamides have been identified with low nanomolar affinity for the V_{1b} receptor and good selectivity with respect to related receptors V_{1a}, V_2 and oxytocin (OT). Optimised compound **12j** demonstrates a good pharmacokinetic profile and activity in a mechanistic model of HPA dysfunction.

© 2010 Published by Elsevier Ltd.

Hyperactivity of the hypothalamic–pituitary–adrenal (HPA) axis is a neuroendocrine abnormality that has been reported to occur in a number of psychiatric conditions.[1] Arginine vasopressin (AVP) and corticotrophin releasing hormone (CRH) are the primary driving forces behind activation of the HPA axis. Both hormones are released from the paraventricular nucleus of the hypothalamus and act in synergy to induce adrenocorticotropic hormone (ACTH) release from anterior pituitary corticotrophs. Both AVP and CRH induce ACTH release through binding to specific G-protein coupled receptors located in the pituitary, the vasopressin V_{1b} (V_3) receptor and CRH_1 receptor. There are strong data to indicate that hyperactivity of the HPA axis during chronic stress and in depression is caused by a shift towards a predominant AVP/V_{1b} regulation of this system.[2] Antagonists of the pituitary (peripheral) V_{1b} receptor are proposed to normalise HPA overactivity and, as such, could provide therapeutic benefit in the treatment of diseases characterised by an excessive cortisol secretion such as major depression and stress-related disorders.[3] Further support for this hypothesis has come from discovery of the V_{1b} antagonist SSR149415. This compound has been proposed to target specifically V_{1b} receptors, since the reported affinities for the related V_{1a}, V_2 and oxytocin (OT) receptors are in the micromolar or submicromolar range.[4] The selectivity of SSR149415 over the other receptor subtypes is high in rat, however, this compound has recently been shown to display significant antagonism of the human (h) OT receptor.[5] SSR149415 has been demonstrated to inhibit AVP-induced ACTH release in vivo and showed activity in animal models predictive of antidepressant and anxiolytic activity after systemic administration. This compound was advanced to Phase IIb clinical trials but appears to have been discontinued.[6]

We recently reported details of our hit-to-lead optimisation effort around a novel series of 2-(4-oxo-2-aryl-quinazolin-3(4*H*)-yl)acetamides as vasopressin V_{1b} receptor antagonists.[7] This effort gave rise to compounds **1** and **2** with good affinity for the human (h) V_{1b} receptor and significantly lower MW and PSA (e.g., **1**, MW = 475, FPSA = 74.37) than other known ligands (Fig. 1). In addition, **1** and **2** demonstrated comparable affinity at the rat (r) V_{1b} receptor and had excellent selectivity for the hV_{1b} receptor vs. the hV_{1a}, hV_2 and hOT receptors. On the basis of their attractive profiles regarding affinity, physicochemical properties and selectivity we initiated a lead optimisation program utilising compounds **1** and **2** as our starting point.

* Corresponding authors. Tel.:+44 7729182555 (S.N.).
E-mail addresses: susannapier67@googlemail.com (S.E. Napier), Jeffrey_letourneau@yahoo.com (J.J. Letourneau).

0960-894X/$ - see front matter © 2010 Published by Elsevier Ltd.
doi:10.1016/j.bmcl.2010.12.081

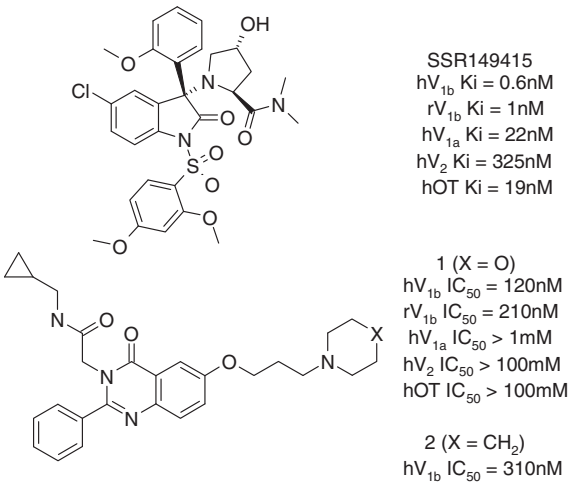

Figure 1. V_{1b} antagonists.

The compounds appearing in Tables 1–3 were synthesised via the general route outlined in Scheme 1. Alternative methods have also been described.[8] 2-Amino-5-hydroxybenzoic acid **3** was reacted with triphosgene to afford the isatoic anhydride **4**. Reaction with glycine amide **5** provided key amide intermediate **6**.[8] Conversion of **6** to intermediate quinazolinones **8** was performed either by condensation of an imidate salt **7** (readily prepared from the corresponding aryl nitrile) or by condensation of **6** with a suitable aldehyde followed by subsequent oxidation of the resultant dihydroquinazolinone intermediate. Finally, the phenol in quinazolinone **8** was alkylated with 1,3-dibromopropane followed by reaction with the appropriate amine to give compounds **9**–**12**.

The compounds in Tables 1–3 were evaluated for their ability to displace the binding of tritium labelled arginine vasopressin ([^{3}H]-AVP) to human V_{1b} receptor in a whole cell binding assay using CHO/human V_{1b}/VIP-Luciferase cells and 5 nM [^{3}H]-AVP.[9] Initially analogues of **1** involving modification to the phenyl substituent at the C(2)-position of the quinazolinone scaffold were explored (Table 1). A systematic scan of the phenyl substituent revealed that substitution was preferred at the 3-position with either electron withdrawing (**9h**) or electron donating (**9g**) groups. Substitution of the phenyl ring at the 4-position was not well tolerated (**9a**–**9d**). Substitution at the 2-position with methyl, to give **9e**, led to a threefold decrease in affinity. Substitution at the 3-position with either a chloro- or methoxy-substituent was favourable for affinity with the 3-chloro analogue **9h** having a fourfold (IC_{50} = 30 nM) and the 3-methoxy analogue **9g** having an eightfold (IC_{50} = 15 nM) higher affinity than **1** (IC_{50} = 120 nM).

Table 1
SAR of phenyl substitution at the C(2)-position of the quinazolinone scaffold

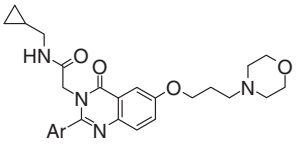

9a-9j

Compds	Ar	hV_{1b} IC_{50}[a] (nM)
1	Ph	120 (±46)
9a	4-Me-phenyl	1450 (±500)
9b	4-MeO-phenyl	1030 (±380)
9c	4-Cl-phenyl	800 (±68)
9d	4-F-phenyl	250 (±180)
9e	2-Me-phenyl	366 (±330)
9f	3-Me-phenyl	125 (±51)
9g	3-MeO-phenyl	15 (±6)
9h	3-Cl-phenyl	30 (±15)
9i	3-F-phenyl	113 (±53)

[a] Values are means of two experiments, standard deviation is given in parentheses.

Table 2
SAR of heteroaryl replacements for phenyl at the C(2)-position of the quinazolinone scaffold

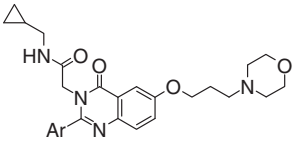

10a-10g

Compds	Ar	hV_{1b} IC_{50}[a] (nM)
1	Ph	120 (±46)
10a	3-Pyridyl	1350 (±780)
10b	4-Pyridyl	3100 (±1600)
10c	2-Thiophenyl	328 (±169)
10d	3-Thiophenyl	470 (±170)
10e	3-Furanyl	644 (±189)
10f	3-Indolyl	387 (±19)
10g	3-Quinolinyl	2400 (±1100)

[a] Values are means of two experiments, standard deviation is given in parentheses.

Replacement of the phenyl moiety with heteroaryl moieties was also investigated (Table 2). Replacement with 3- or 4-pyridyl (**10a** and **10b**) led to a substantial decrease in affinity. Replacement with isosteric 2-thiophenyl, however, gave only a modest decrease with **10c** being only threefold (IC_{50} = 330 nM) less active than **1**. The 3-thiophenyl and 3-furanyl analogues showed similar activity to **10c**. Two analogues (**10f**–**10g**) were prepared in which the phenyl was replaced with bicyclic heteroromatics. Of these **10f** containing a 3-indol-1*H*-yl substituent was the most active, being only three to fourfold less active than **1**.

Next our focus turned to optimisation of the alkyl amide portion of the molecule. Two 2D arrays of twelve compounds each were prepared with the amine substituent fixed as either morpholine (array 1) or piperidine (array 2) since these groups had previously been demonstrated optimal for affinity[7] (Fig. 2). In an effort to

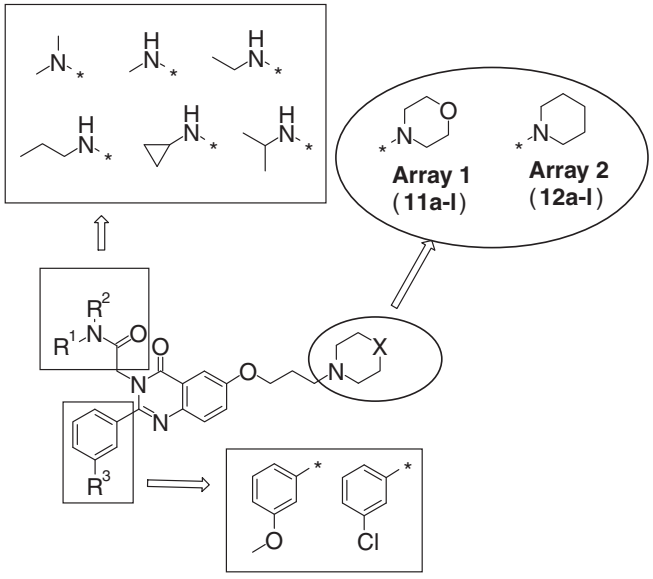

Figure 2. SAR investigation of alkyl amide region in combination with Preferred C(2) aryl and amine substituents.

Table 3
Optimisation of the alkyl amide portion of the molecule prepared as two 2D arrays, **11a–l** and **12a–l**

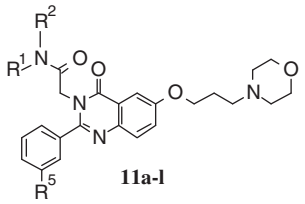

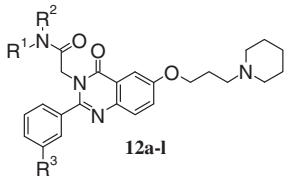

Compds	NR^1R^2	R^5	hV_{1b}, IC_{50}[a] (nM)	HLM[b], rem. @30 min (%)	Compds	NR^1R^2	R^5	hV_{1b}, IC_{50}[a] (nM)	HLM[b], rem.@30 min (%)
11a		OMe	325 (±106)	–	**12a**		OMe	2500 (±71)	–
11b		Cl	6050 (±4313)	–	**12b**		Cl	2350 (±212)	–
11c		OMe	86 (±22)	–	**12c**		OMe	152 (±77)	81
11d		Cl	122 (±22)	–	**12d**		Cl	196 (±40)	64
11e		OMe	42 (±9)	8	**12e**		OMe	72 (±34)	68
11f		Cl	59 (±16)	–	**12f**		Cl	49 (±12)	47
11g		OMe	34 (±11)	–	**12g**		OMe	17 (±11)	81
11h		Cl	26 (±6)	27	**12h**		Cl	46 (±24)	60
11i		OMe	4 (±1)	13	**12i**		OMe	3 (±4)	67
11j		Cl	5 (±1)	9	**12j**		Cl	6 (±1)	57
11k		OMe	>20,000	–	**12k**		OMe	>20,000	–
111		Cl	>20,000	–	**12l**		Cl	>20,000	–

[a] Values are means of two experiments, standard deviation is given in parentheses.
[b] Compound assayed in Human Liver Microsomes in duplicate, percentage compound remaining unchanged after 30 min was determined.

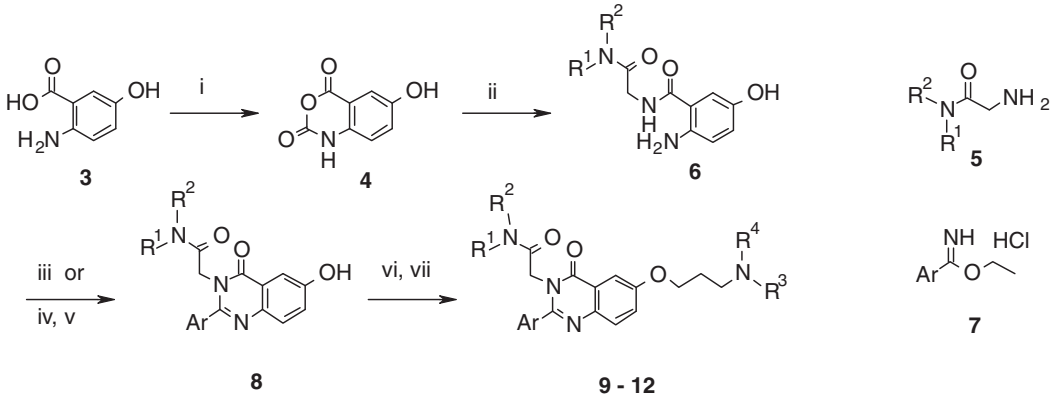

Scheme 1. Reagents and conditions: (i) triphosgene, THF, 0 °C to room temperature; (ii) **5**, CH_3CN, room temperature; (iii) **7**, EtOH; (iv) ArCHO, AcOH (cat.), EtOH, reflux; (v) MnO_2, $CHCl_3$, 60 °C; (vi) 1,3-dibromopropane, K_2CO_3, CH_3CN, reflux; (vii) HNR^3R^4, K_2CO_3, CH_3CN, reflux.

maintain appropriate physicochemical properties in line with known CNS active drugs, we focused our exploration of alternative amide substituents on small (⩽3 carbon) alkyl groups. The C(2) aryl substituents incorporated in each array were either a 3-chloro- or 3-methoxy-substituted phenyl group, as these groups were demonstrated optimal for affinity (vide supra).

Comparable activity was observed between analogous compounds prepared with either morpholine (**11a–l**) or piperidine

(**12a–l**) as amine substituent (Table 3). The nature of the amide substituent, however, had a dramatic impact on affinity. The cyclopropyl amides **11g** (IC_{50} = 34 nM), **11h** (IC_{50} = 26 nM), **12g** (IC_{50} = 17 nM) and **12h** (IC_{50} = 46 nM) had comparable activity to the cyclopropylmethyl analogues **9g** (IC_{50} = 15 nM) and **9h** (IC_{50} = 30 nM). Substitution with *n*-propyl resulted in comparable affinities to cyclopropyl (compare **11g** to **11e**, **11h** to **11f**, **12g** to **12e** and **12h** to **12f**) whereas smaller ethyl (**11c–d**, **12c–d**) or methyl (**11a–b**, **12a–b**) substituents were not well tolerated. In contrast, substitution with a bulky, α-branched isopropyl group gave a four to ninefold increase in affinity (compare **11i** to **11g**, **11j** to **11h**, **12i** to **12g** and **12j** to **12h**) resulting in the identification of four analogues (**11i**, **11j**, **12i** and **12j**) with low nanomolar affinity. Finally, the tertiary dimethylamide analogues (**11k–l**, **12k–l**) were tenfold less potent than the secondary methylamides (**11a–b**, **12a–b**), perhaps indicating the importance of an H-bond donor (i.e., N–H) in this domain.

Assessment of in vitro metabolic stability revealed that analogues containing the morpholine substituent (**11e**, **11h–j**) possessed poor stability in the presence of human liver microsomes (HLM). However, analogues containing the piperidine substituent (**12c–j**) possessed much improved HLM stability indicating that the morpholine substituent itself may be a metabolic liability in this series. Piperidine analogues **12g**, **12i** and **12f** were also tested for stability in the presence of rat liver microsomes (RLM) and demonstrated to have comparable stability to HLM (98%, 65% and 80% remaining in RLM at 30 min, respectively).

Compounds **12i** and **12j**, with low nanomolar affinity and reasonable in vitro metabolic stability in the presence of HLM and RLM, were tested for their affinity at the rat V_{1b} receptor and for selectivity over human V_{1a}, V_2 and OT (Table 4). Comparable affinities were measured for both compounds at human and rat V_{1b} and both compounds demonstrated excellent selectivity (>1000-fold) for the human V_{1b} receptor vs. the related human V_{1a}, V_2 and OT receptors.[10,11] All compounds tested were shown to be V_{1b} antagonists in a luciferase reporter assay linked to AVP-mediated intracellular calcium mobilisation (data not shown). In addition, compound **12j** was submitted for testing against a broad panel of biological targets at Novascreen (GPCRs, ion channels, transporters and enzymes), where it produced less that 50% displacement of binding or inhibition at 2.5 μM.

Table 4
Evaluation of compounds **12i** and **12j** for affinity at rat V_{1b} and human V_{1a}, V_2 and OT receptors vs. affinity at human V_{1b} receptor

Compd	IC_{50}[a] (nM)				
	hV_{1b}	rV_{1b}	hV_{1a}	hV_2	hOT
12i	3	2	>100,000	>100,000	>100,000
12j	6	4	>100,000	>100,000	>100,000

[a] Values are means of at least two experiments

Table 5
Pharmacokinetic parameters for **12i** and **12j** in male Wistar rats

	12i		**12j**	
Route, dose[a]	iv (2 mg/kg)	po (5 mg/kg)	iv (2 mg/kg)	po (10 g/kg)
Clearance (mL/min/kg)	43		36.3	
Elimination half-life (h)	1.2		3.8	
V_{ss} (L/kg)	3.9		9.7	
AUC (ng/mL h)	759	515	980	2565
F%		55		53

[a] Vehicle for both po and iv dosing is 5% (v/v) mulgofen in saline.

The pharmacokinetics after oral and intravenous dosing were determined in male Wistar rats (Table 5). Both **12i** and **12j** showed moderate clearance and high V_{ss}, in the expected range for a basic compound. Moderate clearance and high V_{ss} resulted in moderate to long elimination half-lives of 1.2 h for **12i** and 3.8 h for **12j**. Both compounds had good oral bioavailability (**12i**, *F*% = 55%; **12j**, *F*% = 53%). Additionally the CYP inhibition profiles for **12i** and **12j** were promising (IC_{50} values at main human drug metabolising CYPs >30 μM).

Given its good affinity and favourable PK profile, compound **12j** was selected for further profiling in vivo. **12j** was profiled in a model of HPA hyperactivity.[12,13] Upon administration to rats, desmopressin (dDAVP, a mixed V_{1b}/V_2 agonist) and CRH (a CRH1/CRH2 agonist), work synergistically to elicit the release of ACTH. Pretreatment with a V_{1b} antagonist can attenuate this release of ACTH. Compound **12j** was dosed orally 2 h prior to treatment with dDAVP and CRH. As shown in Figure 3, there was a dose-dependent reduction in ACTH release, indicating that **12j** can antagonise the effects of dDAVP in vivo at 5 mg/kg po.

Compound **12j** was selected for further development and progressed into FIH studies. The human PK parameters for **12j** following dosing at 25 mg po are shown in Table 6. Compound **12j** showed a promising PK profile with a good oral exposure and a half-life suitable for once daily dosing. There was no deviation from dose-proportionality observed over a dose range from 1 to 150 mg.

In conclusion, a series of V_{1b} antagonists exemplified by lead compounds **1** and **2** were further optimised with respect to V_{1b} affinity and in vitro pharmacokinetic profile. Compounds showed good affinity for the rat V_{1b} receptor and high selectivity with respect to V_{1a}, V_2 and OT receptor subtypes and against a broad panel of unrelated targets (Novascreen). The best examples from the series, **12i–j**, exhibited promising pharmacokinetic profiles in rat. Compound **12j** was further profiled in an in vivo model of HPA

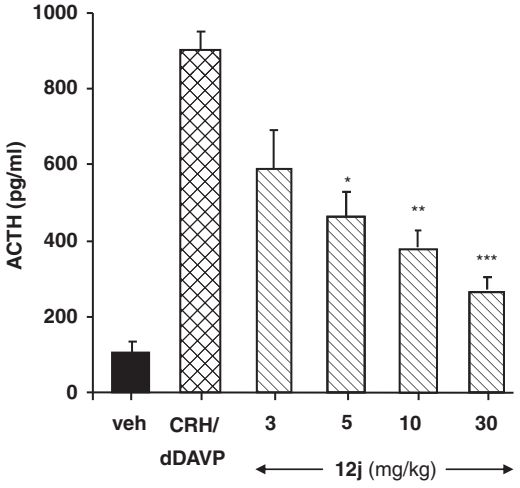

p<0.05; **p<0.005; ***p<0.001 vs CRH/dDAVP

Figure 3. In vivo profiling of **12j** in a rat model of HPA hyperactivity.

Table 6
Pharmacokinetic parameters for **12j** in human volunteers (n = 9) after oral dosing[a]

Compd	C_{max} (ng/mL)	AUC (ng h/mL)	t_{max} (h)	$T_{1/2}$ (h)
12j	79	1013	3.0	11.5

[a] Compound **12j** dosed at 25 mg po (n = 9), vehicle gelatin/mannitol.

hyperactivity where it was demonstrated to antagonise the effects of dDAVP on elevating ACTH levels in rat. Compound **12j** has progressed into clinical development and has been demonstrated to have human PK parameters consistent with once daily dosing. We will report other clinical findings in due course.

References and notes

1. (a) Holsboer, F.; Barden, N. *Endocr. Rev.* **1996**, *17*, 187; (b) Barden, N.; Reul, J. M. H. M.; Holsboer, F. *Trends Neurosci.* **1995**, *18*, 6; (c) Dinan, T. G.; O'Brien, S.; Lavelle, E.; Scott, L. V. *Psychol. Med.* **2004**, *34*, 169.
2. (a) Scaccianoce, S.; Muscolo, L. A. A.; Cigliana, G.; Navarra, D.; Nicolai, R.; Angelucci, L. *Endocrinology* **1991**, *128*, 3138; (b) Ma, X.-M.; Levy, A.; Lightman, S. L. *Endocrinology* **1997**, *138*, 4351.
3. (a) Scott, L. V.; Dinan, T. G. *Life Sci.* **1998**, *62*, 1985; (b) Aquiler, G.; Rabdan-Diehl, C. *Regul. Pept.* **2000**, *96*, 23.
4. (a) Griebel, G.; Simiand, J.; Serradeil-Le Gal, C.; Wagnon, J.; Pascal, M.; Scatton, B.; Maffrand, J.-P.; Soubrie, P. *PNAS* **2002**, *99*, 6370; (b) Serradeil-Le Gal, C.; Wagnon, J.; Tonnerre, B.; Roux, R.; Garcia, G.; Griebel, G.; Aulombard, A. *CNS Drug Rev.* **2005**, *11*, 53.
5. Griffante, C.; Green, A.; Curcuruto, O.; Haslam, C. P.; Dickinson, B. A.; Arban, R. *Br. J. Pharmacol.* **2005**, *146*, 744.
6. ClinicalTrials.gov web-based search. http://clinicaltrials.gov/ct2/search (accessed Aug. 2010), 3 Phase II trials listed using search term 'SSR149415'.
7. Letourneau, J. L.; Riviello, C.; Li, H.; Cole, A. G.; Ho, K.-K.; Zanetakos, H. A.; Desai, H.; Zhao, J.; Auld, D. S.; Napier, S. E.; Thomson, F. J.; Goan, K. A.; Morphy, J. R.; Ohlmeyer, M. H. J.; Webb, M. L. *Bioorg. Med. Chem. Lett.* **2010**, *20*, 5394.
8. Letourneau, J.; Riviello, C.; Ho, K.-K.; Chan, J.-H.; Ohlmeyer, M.; Jokiel, P.; Neagu, I.; Morphy, J. R.; Napier, S. E. PCT Int. Appl. WO 06095014, 2006.
9. *V_{1b} whole cell binding assay*: The assay was performed in a 96-well format. CHO cells stably expressing human V_{1b} receptor were cultured at 37 °C with 5% CO_2 in DMEM/F12 (Invitrogen) with 10% FBS (HyClone Labs, FetalClone II, #206007), 0.4 mg/mL G418 (Invitrogen) and 1% penicillin and streptomycin (Invitrogen). Cells were seeded at 30,000 cells into either 384-well (50 μL/well) or 96-well (100 μL/well) clear bottom plate and cultured at 37 °C overnight. Cells were washed twice with 100 μL/well (for 384-well plate) or 200 μL/well (for 96-well plate) of PBS. For initial HTS, 384-well plates containing dried down compounds were resuspended with 30 μL/well of 5 nM [^{3}H]-AVP in assay buffer (PBS with 10 mM $MgCl_2$, 0.1% BSA and 1% DMSO. After solubilization, 20 μL/well was transferred from compound plate to cell plate. For compound affinity, test compounds were initially serially diluted in DMSO and then intermediately diluted at 1:50 with assay buffer (PBS with 10 mM $MgCl_2$ and 0.1% BSA). To each well, 25 μL of serially diluted compounds were added followed by 25 μL of 10 nM [^{3}H]-AVP in assay buffer. The final reaction contained 5 nM [^{3}H]-AVP and 1% DMSO. The mixtures were incubated at room temperature for 30 min. The plates were washed twice with 100 μL/well (for 384-well plate) or 200 μL/well (for 96-well plate) of PBS and air dried. The amount of radioactivity remaining was determined by adding 50 μL of scintillation fluid and shaking for 30 min followed by counting for 1 min/well in a Perkin–Elmer Microbeta.
10. Human V_2, OT, and rat V_{1b} receptors whole cell binding assays were performed similarly to the human V_{1b} whole cell assay in 96-well format except that CHO cells stably expressing human V_2, OT, and rat V_{1b} receptors were used, respectively. The final reactions contain 5 nM [^{3}H]-AVP for human V_2 and rat V_{1b} receptor assays, and 5 nM [^{3}H]-oxytocin for the human OT receptor assay.
11. Human V_{1a} membrane binding assay performed in 96-well microtitre plates containing (final concentrations): 50 μg/well membrane protein prepared from CHO cells stably expressing human V_{1a} receptor, 5 nM [^{3}H]-AVP and test compounds in a total volume of 100 μL of assay buffer (50 mM Tris–HCl pH 7.4, 5 mM $MgCl_2$, 1 mg/mL BSA, and 0.5% DMSO). The assay mixture was incubated at room temperature for 60 min. The reaction was terminated by rapid filtration of the mixture through 96-well GF/B filters (pre-soaked in 0.3% polyethylenimine) using a Tomtec Harvester. The filters were washed four times with approximately 200 μL of ice-cold 50 mM Tris–HCl (pH 7.4), then dried at 55 °C for 30 min. 50 μL scintillation fluid was then added and the filters counted using a Packard Topcount.
12. Craighead, M.; Milne, R.; Campbell-Wan, L.; Watson, L.; Presland, J.; Thomson, F. J.; Marston, H. M.; MacSweeney, C. P. *Prog. Brain Res.* **2008**, *170*, 527.
13. Rats were orally administered either vehicle (5% mulgofen in saline) or compound at the appropriate dose at $T = 0$. At $T + 100$ min CRH (0.3 μg/kg) or 0.9% phosphate buffered saline (PBS) was administered through a jugular vein catheter. Desmopressin (dDAVP; 0.5 mg/kg) or PBS was administered iv via the catheter at $T + 120$ min. At $T + 130$ min a 0.5 ml blood sample was collected. Samples were stored on ice immediately after collection and then centrifuged (2500 rpm, 4 °C, 15 min). Plasma was extracted and stored at −40 °C. Samples were then analysed for drug and ACTH concentrations by mass spectroscopy and enzyme-linked immunosorbent assay (ELISA: IDS UK), respectively.